Analytical Biochemistry 424 (2012) 12–20

Contents lists available at SciVerse ScienceDirect

Analytical Biochemistry

journal homepage: www.elsevier.com/locate/yabio

Harnessing aptamers for electrochemical detection of endotoxin

Sung-Eun Kim [1], Wenqiong Su [1], MiSuk Cho, Youngkwan Lee, Woo-Seok Choe *

School of Chemical Engineering, Sungkyunkwan University, Suwon 440-746, Republic of Korea

ARTICLE INFO

Article history:
Received 1 January 2012
Received in revised form 7 February 2012
Accepted 8 February 2012
Available online 25 February 2012

Keywords:
Lipopolysaccharide
Aptamer
NECEEM-based non-SELEX
Electrochemical aptasensor

ABSTRACT

Lipopolysaccharide (LPS), also known as endotoxin, triggers a fatal septic shock; therefore, fast and accurate detection of LPS from a complex milieu is of primary importance. Several LPS affinity binders have been reported so far but few of them have proved their efficacy in developing electrochemical sensors capable of selectively detecting LPS from crude biological liquors. In this study, we identified 10 different single-stranded DNA aptamers showing specific affinity to LPS with dissociation constants (K_d) in the nanomolar range using a NECEEM-based non-SELEX method. Based on the sequence and secondary structure analysis of the LPS binding aptamers, an aptamer exhibiting the highest affinity to LPS (i.e., B2) was selected to construct an impedance biosensor on a gold surface. The developed electrochemical aptasensor showed excellent sensitivity and specificity in the linear detection range from 0.01 to 1 ng/mL of LPS with significantly reduced detection time compared with the traditional Limulus amoebocyte lysate (LAL) assay.

Lipopolysaccharide (LPS[2] or endotoxin) is a major component of the outer membrane of gram-negative bacteria [1,2] and induces a strong immune response on its internalization into mammalian cells. When the human circulatory system is infected by LPS, various inflammatory cytokines are overexpressed by activation of the innate immune system and these mediators may render the patient to experience LPS-induced symptoms of septic shock and mortality [3].

Due to its toxicity, the detection and removal of even small amounts of LPS in therapeutic products and blood purification are a primary concern in the treatment of septic shock. Several LPS adsorbents such as activated carbon [4] and polymyxin B [5,6] have been developed for the removal of LPS. Nevertheless, the use of these nonspecific LPS adsorbents usually gives rise to the significant loss of target proteins and/or other nonproteinaceous products (e.g., plasmid DNA) during the removal process [7–10]. Thus ligands capable of specifically recognizing LPS are highly required.

Aptamers are single-stranded oligonucleotides able to bind to a variety of targets including proteins, small molecules, and living cells with high affinity and specificity [11,12]. Ease of synthesis, facile chemical modification, and integration into different analytical schemes have rendered their application in many areas of bioanalytical and biomedical sciences.

Target recognizable aptamers have often been selected from synthetic combinational nucleic acid libraries in general through an *in vitro* selection procedure known as systematic evolution of ligands by exponential enrichment (SELEX) [13,14]. SELEX involves repetitive rounds comprising the following two steps: (1) fractionation of target-bound aptamers from free aptamers and (2) PCR amplification of the selected aptamers. Typically 8 to 15 iterative cycles of partitioning and amplification are required prior to selecting aptamers with high and specific affinity to a target from an initial library [15,16]. As a result, SELEX-based conventional partitioning methods take several months to complete. Moreover, these processes often lead to aptamers that bind to the surface of the filters or chromatographic supports used in partitioning, rather than to the target [17–19].

An alternative screening method termed nonequilibrium capillary electrophoresis of equilibrium mixtures (NECEEM) was proven to have the partitioning efficiency of 2 orders of magnitude higher than that of the conventional methods [20–23]. The outstanding partitioning capabilities of NECEEM have been successfully used in the aptamer selection procedure that does not include intermediate amplification steps between selection rounds (i.e., NECEEM-based non-SELEX) [21]. The obviation of repetitive steps of PCR significantly accelerates the screening process and excludes the quantitative errors associated with the exponential nature of PCR

* Corresponding author. Fax: +82 31 290 7272.
E-mail address: checws@skku.edu (W.-S. Choe).

[1] These authors equally contributed to this work.

[2] *Abbreviations used:* LPS, lipopolysaccharides or endotoxin; K_d, equilibrium dissociation constant; NECEEM, nonequilibrium capillary electrophoresis of equilibrium mixtures; SELEX, systematic evolution of ligands by exponential enrichment; LAL, Limulus amoebocyte lysate; EIS, electrochemical impedance spectroscopy; PCR, polymerase chain reaction; BSA, bovine serum albumin; FAM, fluorescent dye; DTT, 1,4-dithiothreitol; MCH, 6-mercapto-1-hexanol; QCM, quartz crystal microbalance; EU, enzyme unit; EDTA, ethylenediaminetetraacetic acid; RT-PCR, real-time polymerase chain reaction; SPR, surface plasmon resonance; PBS, phosphate-buffered saline; RU, resonance unit; k_a, association constant; k_d, dissociation constant; CV, cyclic voltammetry; R_s, solution resistance; C, double layer capacitance; W, Warburg diffusion resistance; R_{et}, electron transfer resistance; SAM, self-assembled monolayer.

0003-2697/$ - see front matter © 2012 Elsevier Inc. All rights reserved.
doi:10.1016/j.ab.2012.02.016

amplification. This makes non-SELEX a useful tool for selection and characterization of aptamer binders to different targets [22].

Several aptamers have been isolated against LPS for different purposes (e.g., neutralization of the toxicity of LPS [24], inhibition of the growth of *Escherichia coli* [25], and protection of mice from LPS-induced sepsis [26]). However, few aptamer has been tested for its specificity toward LPS in the context of developing an electrochemical sensor capable of selectively detecting LPS from crude biological liquors.

Electrochemical biosensors with the use of modified electrodes via self-assembled monolayers (SAM) have recently attracted much attention [27–29]. Aptamers can be easily modified at their 5′- or 3′-end with various functional groups (e.g., amine, carboxyl, and thiol groups) to facilitate scaffolding of aptamer-modified SAM on a gold electrode surface [30]. Among various electrochemical methods, electrochemical impedance spectroscopy (EIS) is a rapid, sensitive, and nondestructive technique for characterizing the electrochemical property changes at the electrode–electrolyte interfaces and has widely been used as an effective tool for detecting nanogram quantities of biomolecules including bacteria, proteins, DNA, antigens, and antibodies on electrode surfaces [31–33].

In the present study, we have used NECEEM-based non-SELEX to obtain high affinity single-stranded DNA (ssDNA) aptamers to LPS with dissociation constants (K_d) in the nanomolar range. The screened aptamers were thiolated at their 5′-end and used to construct a biosensor where aptamer molecules function as a detection probe to mediate electrochemical impedance changes on their interaction with LPS. The developed electrochemical aptasensor showed a linear detection range from 0.01 to 1 ng/mL of LPS comparable to the traditional Limulus amoebocyte lysate (LAL) assay but with significantly reduced detection time. Furthermore, the developed aptasensor showed negligible cross-binding reactivity to various biomolecules such as pDNA, RNA, proteins, saccharides, and/or lipids which often coexist with LPS in many bioprocessing liquors.

Materials and methods

Materials

LPS from *E. coli* 055:B5 (L4524) was purchased from Sigma-Aldrich (USA). Bare fused-silica capillaries (TSP075375) with a length of 80 cm and inner and outer diameters of 75 and 363 μm, respectively, were purchased from Polymicro (Polymicro Technologies, USA). D-(+)-Glucose (G7021), sucrose (84097), cholesterol (C3045), Baker's yeast RNA (R6750), and bovine serum albumin (BSA, A7906) were from Sigma (St. Louis, MO, USA). Baker's yeast RNA was further purified using LPS removal solution (Sigma, E4274) prior to its use in the experiment. Purified plasmid pDNA pcDNA3.1D was prepared according to the protocol described elsewhere [34].

FAM-labeled random single-strand library (5′-FAM-CTT CTG CCC GCC TCC TTC C-(45N)-GGA GAC GAG ATA GGC GGA CAC T-3′), nonlabeled or FAM-labeled forward primer (5′-CTT CTG CCC GCC TCC TTC C-3′), and nonlabeled or biotin-labeled reverse primer (5′-AGT GTC CGC CTA TCT CGT CTC C-3′) were all synthesized by Integrated DNA Technologies Co., Ltd. (Coraville, USA). Magnetic streptavidin beads (112.05D) were purchased from Invitrogen (Invitrogen Dynal AS, Oslo, Norway). SYBR Green supermix (1708882) was obtained from Bio-Rad (Hercules, USA). Plasmid Mini purification kit (004055) and all the PCR reagents including *Taq* polymerase (CMT 1001) were purchased from LaboPass (Cosmo Genetech, Korea). QIA quick PCR purification kit (28106) was purchased from Qiagen (Hilden, Germany). TA cloning kit (756377) was obtained from Invitrogen (CA, USA). DH5α-competent cells (15045) for cloning were obtained from Intronbio (Seoul, Korea). Limulus amoebocyte lysate assay kit (C1500) was purchased from CapeCod Inc. (East Falmouth, USA). 1,4-Dithiothreitol (DTT) and 6-mercapto-1-hexanol (MCH) were purchased from Sigma-Aldrich. All solutions were prepared using ultrapure water produced by the Satorious Arium 61316 RO system (Sartorius Stedim Biotech, Aubagne Cedex, France).

All the electrochemical experiments were conducted on VSP Potentiostat (Bio-logic Science Instruments, USA) and the data were recorded with VSP EC-Lab software. A conventional three-electrode system with a gold disk electrode of 2 mm diameter (CH Instruments Inc., USA) as the working electrode, an Ag/AgCl as the reference electrode, and a platinum plate as the counterelectrode was employed for all the electrochemical analyses. In EIS measurement, a sine wave of 10 mV amplitude was applied to the working electrode from 0.1 Hz to 100 kHz. The obtained EIS data were calculated by ZSimpWin EIS DATA analysis software (Perkin-Elmer, Version 2.00). Aptamer coverage on the gold surface was measured using Quartz Crystal Microbalance (QCM, Princeton Applied Research, USA) equipped with 10 MHz AT-cut crystals coated with polished gold disk (5 mm in diameter) on both sides under the same conditions used for the gold electrode modification with the aptamer. The frequency change of 1 Hz corresponds to the binding of 1.3 ng of aptamer to the gold disk.

Selection of LPS–affinity aptamer by NECEEM-based non-SELEX

All the screening experiments were conducted using the P/ACE MDQ capillary electrophoresis system (144003, Beckman Coulter) with a LIF detector (727621) following injection of aptamer–LPS mixture at 2 psi for 13 s to a bare fused-silica capillary set at 30 kV and 15 °C. Prior to each run, the capillary was rinsed sufficiently with each of the following solutions: 100 mM HCl, 100 mM NaOH, ultrapure water, and running buffer (50 mM Tris-acetate, pH 8.2).

The FAM-labeled aptamer library (5′-FAM-CTTCTGCCCGCCT-CCTTCC-(45N)-GGAGACGAGATAGGCGGACACT-3′) was diluted in running buffer, heated in a thermal cycler (170-9703, Bio-Rad Laboratories Inc., Hercules, USA) to 95 °C for 1 min and cooled down to 15 °C prior to its injection to the capillary to restore the secondary structure of each ssDNA aptamer in the library. For the screening of LPS affinity aptamers, aptamer–LPS mixture was prepared by mixing 10 μL of 50 μM library with 10 μL of 4 mg/mL (i.e., 2 μM or 2×10^7 EU/mL) of LPS. Following 1 h incubation, 150 nL of the aptamer–LPS mixture was injected to the capillary. During each round of screening, a fraction of the aptamer–LPS complex (designated as Fraction C) was directed to an outlet vial containing 20 μL of 2 mg/mL of fresh LPS solution. Following 1 h incubation, 150 nL of the Fraction C-LPS mixture was injected to the capillary to start a next round of screening. After three rounds of screening, Fraction C from each round of screening (i.e., Fraction C1, C2, or C3) was PCR-amplified and used for assessing the bulk affinity of screened aptamers to LPS.

PCR amplification and purification of ssDNA aptamer

The screened aptamers in Fractions C1 to C3 were PCR-amplified by *Taq* polymerase with the use of nonlabeled forward and biotin-labeled reverse primers in a thermocycler for 30 thermal cycles with each cycle comprising denaturation at 94 °C for 30 s, annealing at 65 °C for 10 s, and extension at 72 °C for 10 s. The amplified biotinylated dsDNA was used as a template for the next asymmetric PCR conducted under the same conditions as above using FAM-labeled forward primer only. The resulting PCR product was incubated with streptavidin-coated magnetic beads for 15 min in binding buffer (100 mM Tris-HCl, 1 mM EDTA, pH 7.5) in order to remove dsDNA. The supernatant containing FAM-labeled

aptamers was collected and further purified using a PCR purification kit. The concentration of purified ssDNA was analyzed by RT-PCR (DNA Engine Peltier Thermal Cycler, Bio-Rad) using SYBR Green supermix.

Cloning and sequencing

The aptamers in Fraction C3 were PCR-amplified by *Taq* polymerase with the use of nonlabeled forward and reverse primers. The amplified products were ligated into PC 2.1 vector provided in TA cloning kit and the ligates were transformed into DH5α-competent cells. Plasmids extracted from 32 transformants using a plasmid purification kit were sent for sequencing.

Determination of dissociation constant (K_d)

Cloned aptamers or the aptamers in Fractions C1 to C3 were amplified, purified, and quantified as described above. To assess the binding affinity of screened aptamers to LPS, 10 μL of 60 nM of each aptamer was mixed with 10 μL of 4 mg/mL LPS in running buffer for 1 h and 150 nL of the incubated mixture was injected to the capillary. The CE running condition was the same as described above. Assessment of K_d was conducted based on the determination of peak areas accounting for LPS–DNA complex (A1), DNA dissociated from complex (A2), and free DNA (A3) as shown in Eq. (1) [23] and Fig. 1 (adopted and modified from Ref. [23]).

$$K_d = \frac{[\mathrm{LPS}]_{tot}\left(1+\frac{A_3}{A_1+A_2}\right) - [\mathrm{DNA}]_{tot}}{\left(1+\frac{A_1+A_2}{A_3}\right)}, \quad (1)$$

where $[\mathrm{LPS}]_{tot}$ and $[\mathrm{DNA}]_{tot}$ are the total concentrations of the LPS and aptamer, respectively.

Surface plasmon resonance (SPR) analysis to study the interaction between thiol-modified, immobilized aptamer B2 and LPS

To verify if the high affinity binder B2 keeps its LPS recognition ability following thiol modification at the 5′ end of the aptamer molecules and their subsequent immobilization onto the gold electrode, SPR analysis was performed to determine the equilibrium dissociation constant (K_d) for thiolated/immobilized B2–LPS interaction. All SPR experiments were conducted on a Reichert SR7500DC instrument and two-channel (i.e., a ligand and a reference channel, respectively) gold chips (13206060, Reichert, NY, USA) using PBS (10 mM, pH 7.4) as running buffer. The bare chips were cleaned in piranha solution (H_2SO_4/H_2O_2 (3/1)) for 15 min, thoroughly washed with ultrapure water, sonicated in ultrapure water and ethanol for 1 min each, and dried under nitrogen. Aptamer molecules were immobilized on the ligand channel by injecting 200 nM of thiolated B2 in PBS to the channel followed by 4 h incubation. Subsequently the chip was immersed in 1 mM MCH/PBS for 2 h to block the aptamer unloaded chip surfaces on the ligand and reference channels. After washing the chip surface with PBS, each LPS/PBS solution prepared at varying concentrations (0.005, 0.01, 0.02, and 0.04 mg/mL) was injected sequentially into both channels for 240 s at a flow rate of 20 μL/min. Between each LPS injection, the channels were washed with PBS for 180 s. LPS–aptamer interaction was monitored based on the difference of response unit (ΔRU) between the ligand channel and reference channel. The ΔRU data were fitted to a kinetic titration 1:1 interaction model using CLAMP (Center for Biological Interaction Analysis, UT, USA). The association and dissociation constants (i.e., k_a and k_d, respectively) were determined from the fit to obtain the equilibrium dissociation constant (K_d).

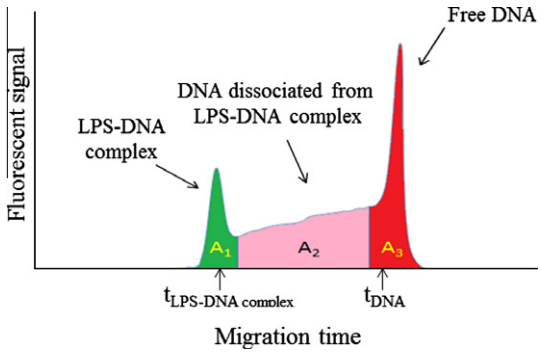

Fig.1. A schematic of a putative electropherogram from NECEEM following the injection of ssDNA aptamer library and LPS mixture. Al, A2, and A3 represent the peak areas for LPS–DNA complex, DNA dissociated from the complex, and free DNA, respectively.

Detection of LPS using aptamer-modified gold electrodes

An aptamer B2 exhibiting the highest affinity to LPS and a control aptamer C2 lacking affinity to LPS were modified by Integrated DNA Technologies to introduce a disulfide modifier at the 5′ end of each. In order to enable self-assembly of thus obtained aptamers on a gold surface, the disulfide group was reduced by DTT for 1 h at room temperature [35] to give 5′ sulfurhydryl-terminated aptamer (5′-HS–$(CH_2)_6$–). Following the reaction, the thiolated aptamer was purified by centrifugal filter (UFC900324, Millipore) at 10,000*g* for 30 min (×3) and the purified aptamer was diluted by PBS (10 mM, pH 7.4) to give an aptamer concentration of 11.5 nM based on UV absorption at 260 nm.

Gold disk electrodes were prepared according to the protocol described elsewhere [36] and then electrochemically activated by cyclic voltammetry (CV) in 0.5 M H_2SO_4 aqueous solution from 0 to 1.5 V at a rate of 100 mV/s for 20 cycles. Afterward, the electropolished electrodes were dried and immediately immersed in the PBS containing thiolated aptamer for 3 h at room temperature. The aptamer-modified gold electrode was incubated in 1 mM MCH aqueous solution for 1 h at room temperature [37]. EIS measurement in 2 mM $Fe(CN)_6^{3-/4-}$ (1/1)/PBS was conducted to electrochemically assess interaction of the aptamer-modified gold electrode with varying amounts of LPS. As a control, EIS measurement was repeated for other biomolecules (e.g., pDNA, RNA, proteins, saccharides, and lipids) often found in biological liquors where LPS is likely to exist in order to evaluate the specificity of the sensor. Unless otherwise noted, all the EIS measurements were conducted after immersing the electrodes in the corresponding solutions for 15 min.

Results and discussion

Selection of LPS affinity aptamers

In order to screen aptamers showing high affinity to LPS using NECEEM, it is important to define a collection window where the LPS–aptamer complex is likely to be populated. For this, migration times of free LPS and free ssDNA library were determined under the CE running condition. Since LPS gave no apparent UV or fluorescence signal, its migration time was estimated by collecting LPS in six fractions (from 0 to 48 min, 8 min/fraction) and quantifying LPS in each fraction by LAL assay. It was found that approximately 80% of the injected LPS molecules were distributed in the fractions collected from 8 to 24 min following their injection. The migration time of FAM-labeled free ssDNA library, monitored by LIF, was found to be around 34 min. When the equilibrium mixture

comprising 25 μM FAM-labeled ssDNA library and 2 mg/mL of LPS was injected to the capillary, several low intensity peaks, in addition to the free ssDNA peak, were observed on the electropherogram between 21 and 27 min (Fig. 2). The migration window for these peaks was located between those for free LPS and ssDNA library, accounting for the presence of putative LPS-aptamer complexes in the equilibrium mixture. To ensure the efficient recovery of ssDNA complexed with LPS, all the aptamers present in an aptamer collection window from 20 to 31 min were directed to a reservoir containing 2 mg/mL of fresh LPS in 20 μL running buffer in order to expedite the next round of selection. Following 1 h incubation, this equilibrium mixture was then injected to the capillary to start the second round of screening. In this study, three rounds of selection were conducted and the collected aptamer pools from each round (i.e., Fractions C1, C2, and C3) were used to assess the bulk affinity of screened aptamers to LPS. Each fraction containing enriched LPS affinity aptamers was amplified by PCR, purified, and quantified by RT-PCR. Ten microliters of 60 nM of these aptamers was mixed with 10 μL of 4 mg/mL of fresh LPS solution and 150 nL of this mixture was injected to the capillary.

A peak corresponding to LPS–aptamer complex was observed in a time window 25–30 min in front of a small peak accounting for free DNA around 32–34 min (Fig. 3). Using Eq. (1), the equilibrium dissociation constant (K_d) for the interaction between the enriched aptamer pools and the LPS was determined from the analysis of peak areas for LPS-aptamer complexes and free DNA (Fig. 4). It was found that the bulk K_d measured for the fractionated aptamer pool following each round of selection decreased with selection rounds, indicative of the successful enrichment of aptamers with enhanced affinity to the target. In addition, the bulk affinity of aptamers evolved after the third round of selection showed no further difference when compared to that from the second round, confirming that three rounds of NECEEM-based non-SELEX should be sufficient to obtain high affinity aptamers to LPS.

Assessment of K_d for the screened LPS affinity aptamers

Following the three rounds of selection, 32 clones harboring the PCR-amplified LPS affinity aptamers ligated into PC 2.1 plasmid were sampled and their DNA sequences analyzed. Table 1 shows the aptamer sequences recovered from 32 clones. For simplicity, each LPS affinity aptamer is designated as B1 to B10. It is noted that B1 dominated Fraction C3 with 23 copies out of 32 ssDNA aptamer sequences.

The homology of the LPS binding aptamers listed in Table 1 was analyzed by DNAman and found to be around 49.4% (Fig. 5A). Surprisingly, the LPS binders B1, B2, B3, and B4 showed more than 98% identity in their nucleotide sequences, indicating that these four binders essentially evolve from a highly conserved sequence (i.e., TAGCCGGATCGCGNTGGCCAGATGATATAAAGGGTCANCCCCCCN, where N denotes any of the four nitrogenous bases) conducive to exhibiting specific affinity to LPS (Fig. 5B).

The relative affinities of the screened aptamers to LPS were judged based on the K_d values estimated for individual LPS binders using Eq. (1). As shown in Table 1, K_d values for the majority of 10 LPS binders were found to be in nanomolar range, suggesting that most of the selected sequences exhibit significantly high affinity to LPS as compared with the controls. It is also noted that B1, B2, B3, and B4 exhibit similar high affinity to LPS as anticipated from their high sequence homology reported in Fig. 5B. This further confirms that the consensus sequence plays an important role in LPS recognition and binding of these four binders. Interestingly, B9, which also shows a low K_d of 15 nM, exhibits only 32–34% sequence homology with B1 to B4 analogues, suggesting that B9 may be an independent LPS binder evolved from a different ssDNA origin. The negative controls (i.e., the ssDNA aptamer library and/or an unbound ssDNA sequence eliminated from the screening at an early stage) showed no binding to LPS.

Putative secondary structures of each LPS binding aptamer were predicted by submitting the corresponding aptamer sequences to the Mfold web server [38]. As shown in Table 2, a common secondary structure resembling "M-shape" was found for B1 to B3 binders, further confirming that the high sequence homology among these binders allows them to have a conservative structural fit conducive to recognizing LPS. Despite the high sequence homology (e.g., B4) or the comparable low dissociation constant (e.g., B9), B4 and B9 showed several putative secondary structures departing from those predicted for B1 to B3, suggesting that LPS recognition by B4 or B9 might be mediated via differential mechanisms in the context of either structural and/or sequence fit.

Taken together, NECEEM was successfully introduced into the non-SELEX process to greatly facilitate the screening of high affinity aptamers to LPS in a few days in contrast to the conventional SELEX usually requiring several months to complete 8 to 15 rounds

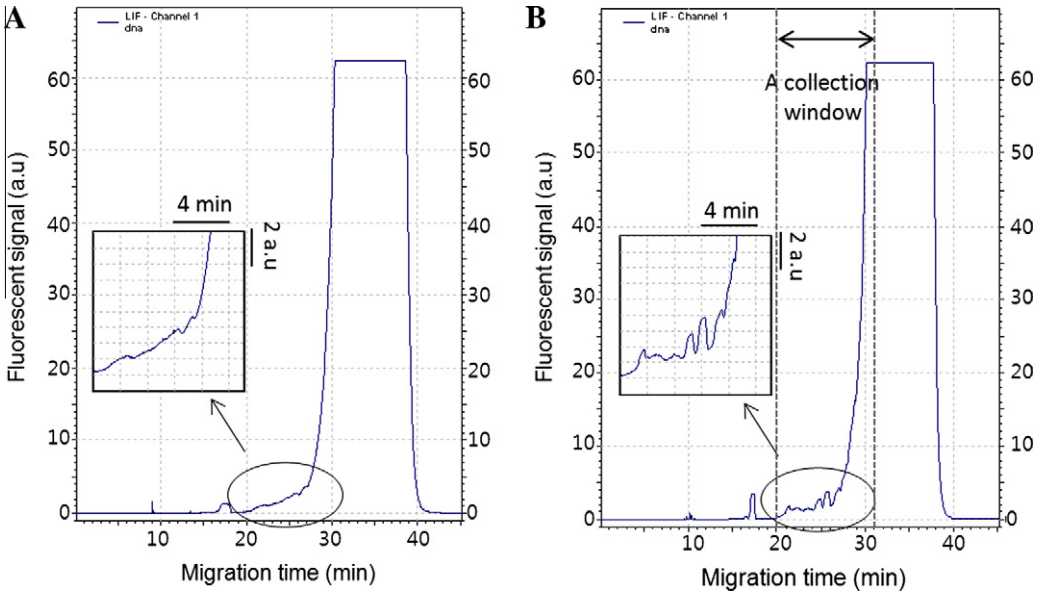

Fig.2. Electropherograms for (A) 25 μM ssDNA library; (B) equilibrium mixture of 25 μM ssDNA library and 2 mg/mL LPS after 1 h incubation.

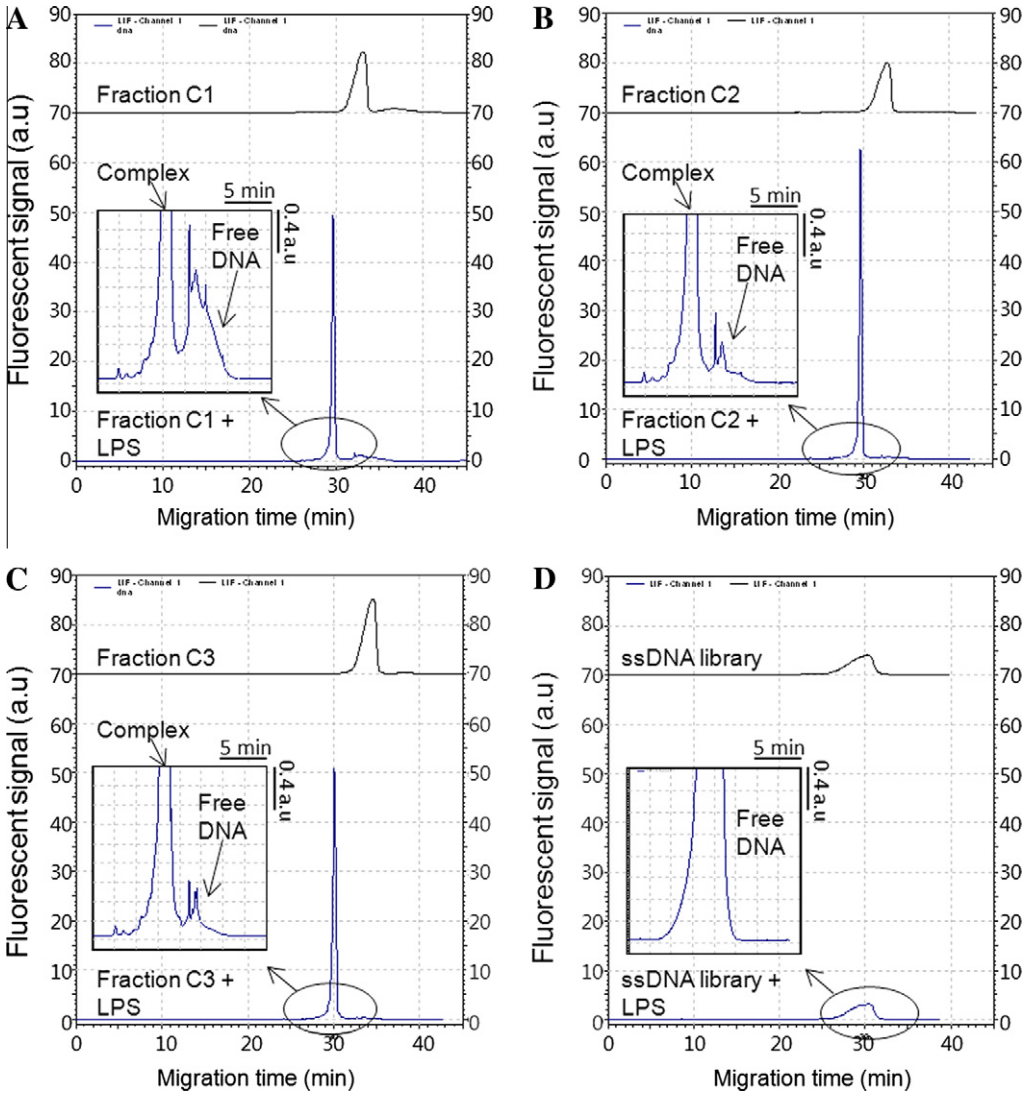

Fig.3. Electropherograms of equilibrium mixture between LPS and (A) Fraction C1, (B) Fraction C2, (C) Fraction C3, (D) ssDNA library.

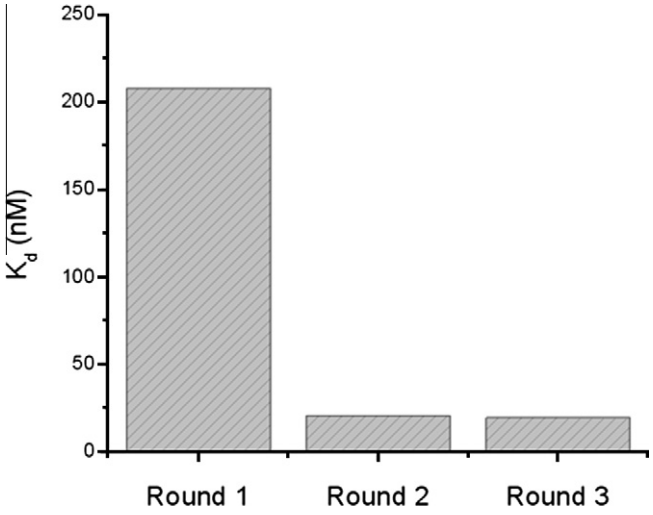

Fig.4. K_d assessed for the enriched aptamer pools during the three rounds of screening against LPS.

of repeated screening. More importantly, NECEEM-based non-SELEX was conducted in solution where the natural configurations of the target molecule and aptamer library members could be effectively retained. This would decrease the chances of nonspecific bindings of aptamers to the surface of the solid supports (e.g., filters or chromatographic matrices) often used in the conventional partitioning methods to immobilize target molecules, thereby resulting in significant affinity enhancement of the initial DNA library just after three rounds of selection.

In order to explore the possibility of harnessing LPS binding aptamers for construction of an electrochemical aptasensor capable of detecting LPS from complex biological liquors, at least two factors (i.e., sensitivity and specificity) must be considered. On the basis of the aforementioned sequence and structure analysis for the 10 LPS binding aptamers, the highest LPS affinity binder B2 was therefore selected to see if aptamer molecules function as a sensor probe to mediate electrochemical impedance changes on their interaction with LPS.

Construction of the aptasensor and assessment of its performance

The B2 binder was modified with a thiol group ($HS–(CH_2)_6–$) at its 5′ terminal to facilitate its anchoring to the gold electrode surface. Prior to constructing an aptasensor where the aptamer B2 on the electrode works as a detection probe, it is important to confirm

Table 1
Aptamer sequences screened against LPS and K_d of each aptamer estimated using Eq. (1).

ID	Sequence	Frequency	K_d (nM)
B1	H[a]-TAGCCGGATCGCGCTGGCCAGATGATATAAAGGGTCAACCCCCCA-T[a]	23	20
B2	H-TAGCCGGATCGCGCTGGCCAGATGATATAAAGGGTCAGCCCCCCA-T	1	12
B3	H-TAGCCGGATCGCGTTGGCCAGATGATATAAAGGGTCAACCCCCCA-T	1	32
B4	H-TAGCCGGATCGCGCTGGCCAGATGATATAAAGGGTCAACCCCCCG-T	1	21
B5	H-CTAAGCACAGGGAAACCAGCTAATGAGTTAGGCCTGTCCCCCACG-T	1	484
B6	H-CAATGGACCTATTCGAGTACTGAATAGAACAGTCGGCGCTCTGGG-T	1	298
B7	H-TTCAAGACGATGCCTGGCGCGAGTTACACACTTGCATGGAGCTGG-T	1	61
B8	H-ATCCAATACCTCAGAACTCAGTTCGAGTCGTAAAGGGGAATCGCA-T	1	71
B9	H-ACCGATCCATCGAGTTTCTGAGAAAGGCCCGGAGAAACCGCGAGA-T	1	15
B10	H-TCAATCTAACCATGCATGCAGTTTAGGCAGGATTCGTTATCGCAA-T	1	2336
Control1[b]	H-(45N)-T		–[d]
Control2[c]	H-GTCATGCTCGAGTCAGGGGTTAGTAAGTCGACGGTACTACGGGAA-T		–[d]

[a] Constant Head (H) and Tail (T) sequence regions flanking the randomized 45-mer ssDNA. H and T represent CTTCTGCCCGCCTCCTTCC and GGAGACGAGATAGGCGGACACT, respectively.
[b] Control 1 (C1) is the randomized aptamer library used for first round of screening.
[c] Control 2 (C2) is recovered from the unbound fraction of ssDNA library after the first round of NECEEM-based screening, hence expected to have no affinity to LPS.
[d] K_d values for the control sequences are unable to be determined due to their negligible interaction with LPS.

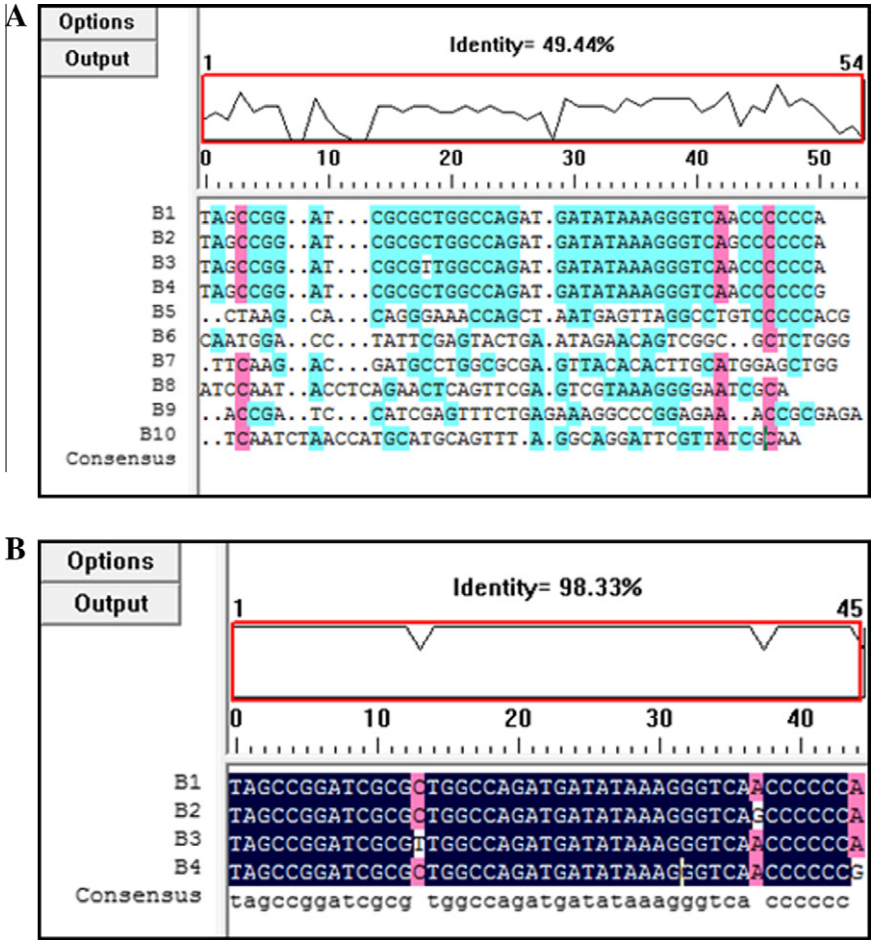

Fig.5. Homology analysis with DNAman for (A) the 10 LPS binding aptamers and (B) the selected 4 binders (i.e., B1 to B4).

if the B2 would preserve its LPS recognition ability following its modification and/or immobilization onto the gold electrode. In order to address this issue, the affinity of B2 binder to LPS was reassessed using an independent technique using surface plasmon resonance (SPR) where the interaction between the thiol-modified B2 aptamer immobilized on the gold chip and LPS in running buffer could be monitored quantitatively. The SPR-based K_d between the immobilized B2 and the LPS was found to be approximately 38 nM. This is very close to the aforementioned CE-based K_d value of 12 nM, indicating that either the free or the immobilized B2 after its thiol modification at 5′ terminal interacts with LPS more or less to the same extent in the nanomolar range. It is therefore concluded that the screened aptamer B2 retains its high affinity to LPS molecules following its modification and immobilization on a gold surface, thereby likely to act as an LPS-sensing element.

An aptasensor harnessing the B2 aptamer as an LPS probe was fabricated as described under Materials and methods. During modification of the gold electrode, cyclic voltammetry (CV) measurements in 2 mM $K_3Fe(CN)_6$ aqueous solution containing 0.1 M KCl were conducted in the range of −0.3 to 0.6 V at a scan rate of

Table 2
Putative secondary structures of each LPS bindng aptamer predicted by Mfold DNA and assessment of sequence homology of each LPS binder against the strongest LPS binder B2.

ID	Predicted secondary structures[a]	Homology to B2 (%)
B1		97.78
B2	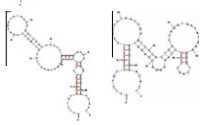	–
B3	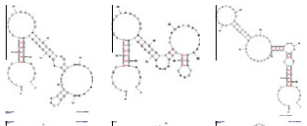	95.56
B4	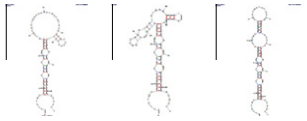	95.56
B5	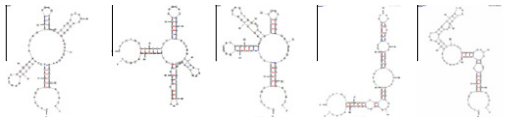	42.55
B6	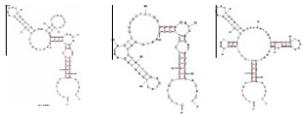	38.30
B7	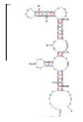	32.61
B8	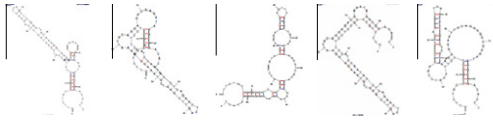	30.00
B9	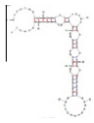	31.91
B10	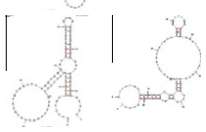	40.43

[a] The structures for each LPS binder are arranged based on their predicted Gibbs free energy in ascending order.

100 mV s^{-1} to characterize the changes on the electrode surface. After immobilization of aptamer molecules followed by MCH blocking, the redox peak showed a corresponding significant decrease for each modification step. This demonstrates that the gold surface was mostly covered by the mixed self-assembled monolayer of aptamer and MCH. Aptamer density on the gold electrode was measured by QCM and found to be 2.0 ng/mm^2 (data not shown).

The surface properties of the modified electrode have been characterized by EIS. A typical impedance spectrum (presented in Nyquist plot) comprises a semicircled high frequency and linear low frequency regions accounting for electron-transfer and diffusion-limited processes, respectively. The electrode/electrolyte interface impedance has been approximated by an equivalent circuit with mixed kinetics and charge transfer control comprising the solution resistance (R_s), the double layer capacitance (C), the Warburg diffusion resistance (W), and the electron-transfer resistance (R_{et}) [33] to fit the electron transfer kinetics of the redox couples (i.e., $Fe(CN)_6^{3-/4-}$) at the interface. The model-based regression and experimental results showed good agreements over the 0.1 Hz and 100 kHz frequency range. The Nyquist plots for a gold electrode at each stage of the surface treatment (i.e., aptamer conjugation followed by MCH blocking) are shown in Fig. 6A (i.e., curves 1–3).

The bare gold electrode exhibits an almost straight line with a negligible semicircle observed at a very high frequency region in the Nyquist plot of impedance spectroscopy (Fig. 6A, curve 1), indicating that a diffusion-controlled process is dominant for the entire frequency range explored. Following deposition of aptamer molecules on the gold electrode, an obvious semicircle indicative of the onset of charge-transfer-controlled process (Fig. 6A, curve 2) appeared. However, it is noted that the contribution of diffusion-controlled process still persists at the low frequency region. This indicates a successful formation of an aptamer layer on the electrode which apparently acted as a barrier for the electrolytes (i.e., $Fe(CN)_6^{3-/4-}$ ions) to access the electrode surface due to the presence of a large number of negatively charged phosphate groups in the adsorbed aptamer layer [27]. When the aptamer-modified gold electrode was further treated with MCH solution, the larger semicircle in the Nyquist plot (Fig. 6A, curve 3) evidencing the formation of a mixed self-assembled monolayer of the aptamer and the spacer thiol was observed. This monolayer on the electrode works against migration and/or mass transfer of electrons from the bulk solution to the electrode surface by further insulating the conductive support and hindering the access of redox probe toward the electrode surface, thereby resulting in a significant increase in R_{et} [39].

Herne and Tarlov [37] have extensively characterized the two-step method to immobilize ssDNA probes on gold surfaces. They reported that the posttreatment with MCH largely replaced disoriented nonspecifically positioned aptamers (i.e., those attached on the electrode surface through nitrogenous base or sulfur atom-mediated physisorption), facilitating precise orientation of ssDNA molecules. Besides, the addition of a large number of MCH molecules rendered topologically favored surface spread ssDNA molecules in a horizontal configuration oriented in axial direction, giving rise to a tightly packed aptamer/MCH mixed layer likely to pose a high steric and electrostatic hindrance to redox ions in accessing the electrode surface [40].

Following the formation of a stable aptamer/MCH mixed layer on the gold electrode, the aptamer-coupled electrode was used to detect LPS at varying concentrations (0.01, 0.1, 0.25, 0.5, 0.75, and 1 ng/mL) in PBS by EIS measurement. As shown in Fig. 6A (curves 4–9) and Fig. 6B, the increase in R_{et} is proportional to the LPS concentration with R^2 coefficient >0.99 in the range of 0.01–1 ng/mL (i.e., 0.05–5 EU/mL), which is comparable to the LPS detection range (i.e., 0.05–5 EU/mL) reported by the conventional LAL assay. Moreover, the time required for LPS detection by the demonstrated aptasensor is no longer than 15 min as compared to 1.5–2.0 h for the LAL assay. The results in Fig. 6 clearly show that the screened aptamer molecule B2 is functional in recognizing LPS following its conjugation to the gold electrode, and able to mediate electron-transfer resistance change (ΔR_{et}) sufficient to detect femtomolar levels of LPS in the solution.

Since LPS is one of the more abundant molecules present in the outer membrane of gram-negative bacteria, many other host cell-derived components such as sugars, lipids, nucleic acids, and proteins are likely to coexist with LPS in a majority of biological liquors from which purification of a target bioproduct (e.g., therapeutic proteins, plasmid DNA vaccines, cytokines) is often attempted. For a practical implementation of the developed LPS

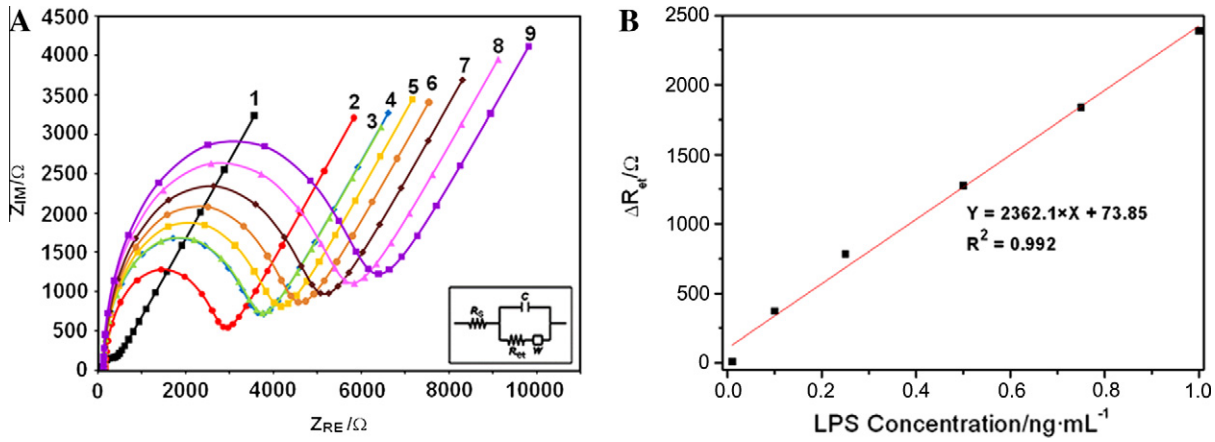

Fig.6. (A) Nyquist plots for the gold electrode during modification (1–3: bare, aptamer deposition, MCH deposition) and detection (4–9: 0.01, 0.1, 0.25, 0.5, 0.75, and 1 ng/mL of LPS) processes and the equivalent circuit (inner) used to model EIS data. (B) The linear relationship between ΔR_{et} and LPS concentration.

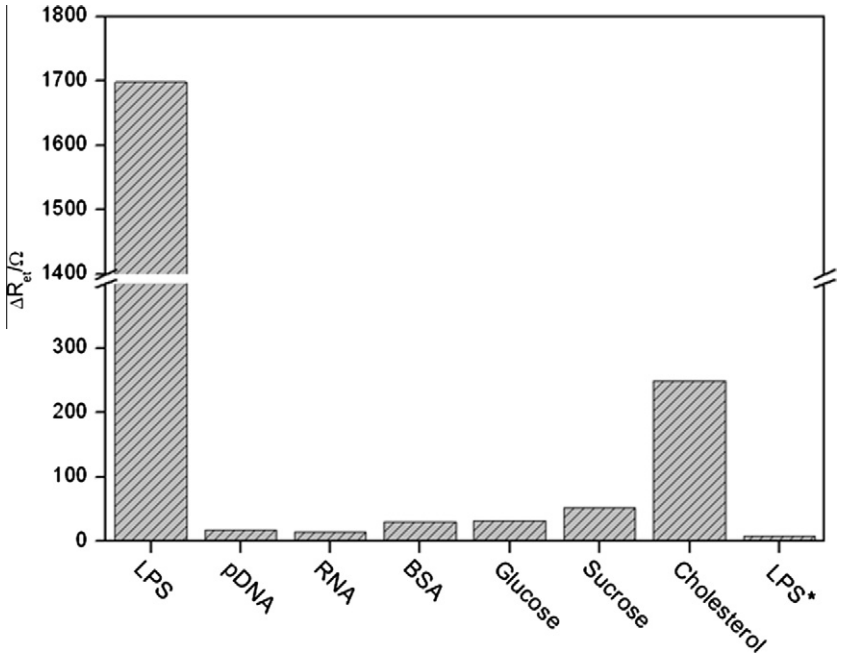

Fig.7. The electron-transfer resistance (ΔR_{et}) calculated from the EIS data recorded after incubation of the aptasensors with LPS (1 ng/mL), pDNA (100 ng/mL), RNA (25 μg/mL), BSA (50 μg/mL), glucose (50 μg/mL), sucrose (50 μg/mL), and cholesterol (50 μg/mL). An aptasensor employing the control aptamer (C2) showed virtually no interaction with 1 ng/mL of LPS as shown in LPS* column. ΔR_{et} represents the change in R_{et} of the aptasensors after 15 min incubation with the various analytes.

aptasensor to the downstream bioprocess, it is therefore important to determine how specifically the aptasensor interacts with LPS without exhibiting cross-binding affinity to other biomolecules. In order to assess the sensor performance in view of selective LPS detection, pDNA, RNA, BSA, glucose, sucrose, and cholesterol were selected as the representative model analytes most likely to be found in a LPS-rich milieu. As summarized in Fig. 7, the developed aptasensor showed negligible cross-reactivity (i.e., almost no ΔR_{et}) to pDNA, RNA, BSA, glucose, or sucrose despite their high concentrations (i.e., 100–50000 times higher than LPS concentrations used for the test). Even though the ΔR_{et} obtained from cholesterol is a little higher than the other analytes tested, considering that a 50,000 times higher (as compared to LPS) concentration of cholesterol was used for the measurement, this result is still able to demonstrate that the aptasensor is highly selective in interacting with LPS and hence compatible with complex bioprocessing liquors.

To further demonstrate the specificity of the LPS aptamer, the control aptamer (i.e., C2 in Table 1) lacking affinity to LPS was anchored to a gold electrode following the same procedure applied to B2. From Fig. 7, it is evident that LPS detection by the aptasensor is solely mediated by the presence of a high affinity LPS binder B2 since the EIS response on incubation of the control aptasensor with LPS showed a negligible ΔR_{et}.

Conclusions

A high affinity LPS binder B2 was identified by a NECEEM-based non-SELEX method. To explore the possibility of harnessing B2 aptamer as a specific sensor probe to detect LPS in solution, an electrochemical apatasensor based on aptamer/MCH-mixed SAM on the gold electrode was fabricated. The developed aptasensor was demonstrated to detect LPS at a range of 0.01–1 ng/mL (i.e., at a femtomolar level comparable to the conventional LAL assay) in 15 min. Furthermore, the aptasensor showed little cross-interaction reactivity to plasmid DNA, RNA, proteins, saccharides, and/or lipids which are most likely to coexist with LPS in a majority of

biological liquors, providing a good potential in realizing practical applications of the developed aptasensor to crude biological liquors where a rapid and specific detection of LPS is of primary concern.

Acknowledgments

This work was supported by research Grants (NRF-C1AAA001–2011-0018903) through the National Research Foundation of Korea (NRF) funded by the Ministry of Education, Science, and Technology (MEST), Korea.

References

[1] A. Preston, R.E. Mandrell, B.W. Gibson, M.A. Apicella, The lipooligosaccharides of pathogenic gram-negative bacteria, Crit. Rev. Microbiol. 22 (1996) 139–180.
[2] R.J. Ulevitch, P.S. Tobias, Receptor-dependent mechanisms of cell stimulation by bacterial endotoxin, Annu. Rev. Immunol. 13 (1995) 437–457.
[3] Y.G. Kim, C.S. Lee, W.J. Chung, E.M. Kim, D.S. Shin, J.H. Rhim, Y.S. Lee, B.G. Kim, J. Chung, Screening of LPS-specific peptides from a phage display library using epoxy beads, Biochem. Biophys. Res. Commun. 329 (2005) 312–317.
[4] J.P. Nolan, J.J. McDevitt, G.S. Goldmann, C. Bishop, Endotoxin binding by charged and uncharged resins, Proc. Soc. Exp. Biol. Med. 149 (1975) 766–770.
[5] A.C. Issekutz, Removal of gram-negative endotoxin from solutions by affinity chromatography, J. Immunol. Methods 61 (1983) 275–281.
[6] S. Minobe, T. Sato, T. Tosa, I. Chibata, Characteristics of immobilized histamine for pyrogen adsorption, J. Chromatogr. A 262 (1983) 193–198.
[7] F.B. Anspach, O. Hilbeck, Removal of endotoxins by affinity sorbents, J. Chromatogr. A 711 (1995) 81–92.
[8] T.E. Karplus, R.J. Ulevitch, C.B. Wilson, A new method for reduction of endotoxin contaminations from protein solutions, J. Immunol. Methods 105 (1987) 211–220.
[9] I.P. Wicks, M.L. Howell, T. Hancock, H. Kohsaka, T. Olee, D.A. Carson, Bacterial lipopolysaccharide copurifies with plasmid DNA: implications for animal models and human gene therapy, Hum. Gene. Ther. 6 (1995) 317–323.
[10] P.M. Montbriand, R.W. Malone, Improved method for the removal of endotoxin from DNA, J. Biotechnol. 44 (1996) 43–46.
[11] D.S. Wilson, J.W. Szostak, In vitro selection of functional nucleic acids, Annu. Rev. Biochem. 68 (1999) 611–647.
[12] M. Famulok, G. Mayer, M. Blind, Nucleic acid aptamers-from selection in vitro to applications in vivo, Acc. Chem. Res. 39 (2000) 591–599.
[13] A. Ellington, J. Szostak, In vitro selection of RNA molecules that bind specific ligands, Nature 346 (1990) 818–822.
[14] C. Tuerk, L. Gold, Systematic evolution of ligands by exponential enrichment: RNA ligands to bacteriophage T4 DNA polymerase, Science 249 (1990) 505–510.
[15] B. Vant-Hull, A. Payano-Baez, R.H. Davis, L. Gold, The mathematics of SELEX against complex targets, J. Mol. Biol. 278 (1998) 579–597.
[16] Y. Tian, N. Adya, S. Wagner, C.Z. Giam, M.R. Green, A.D. Ellington, Dissecting protein:protein interactions between transcription factors with an RNA aptamer, RNA 1 (1995) 317–326.
[17] D. Schneider, L. Gold, T. Platt, Selective enrichment of RNA species for tight binding to *Escherichia coli* rho factor, FASEB J. 7 (1993) 201–207.
[18] H. Chen, L. Gold, Selection of high-affinity RNA ligands to reverse transcriptase: inhibition of cDNA synthesis and RNase H activity, Biochemistry 33 (1994) 8746–8756.
[19] A. Petrov, V. Okhonin, M. Berezovski, S.N. Krylov, Kinetic capillary electrophoresis (KCE): a conceptual platform for kinetic homogeneous affinity methods, J. Am. Chem. Soc. 127 (2005) 17104–17110.
[20] A.P. Drabovich, M. Berezovski, V. Okhonin, Selection of smart aptamers by methods of kinetic capillary electrophoresis, Anal. Chem. 78 (2006) 3171–3178.
[21] M. Berezovski, M. Musheev, A. Drabovich, S.N. Krylov, Non-SELEX selection of aptamers, J. Am. Chem. Soc. 128 (2006) 1410–1411.
[22] M.V. Berezovski, M.U. Musheev, A.P. Drabovich, J.V. Jitkova, S.N. Krylov, Non-SELEX: selection of aptamers without intermediate amplification of candidate oligonucleotides, Nat. Protoc. 1 (2006) 1359–1369.
[23] M. Berezovski, A. Drabovich, S.M. Krylova, M. Musheev, V. Okhonin, A. Petrov, S.N. Krylov, Nonequilibrium capillary electrophoresis of equilibrium mixtures: a universal tool for development of aptamers, J. Am. Chem. Soc. 127 (2005) 3165–3171.
[24] J.L. Ding, S.T. Gan, B. Ho, Single-stranded DNA oligoaptamers: molecular recognition and LPS antagonism are length- and secondary structure-dependent, J. Innate Immun. 1 (2009) 46–58.
[25] J.G. Bruno, M.P. Carrillo, T. Phillips, In vitro antibacterial effects of antilipopolysaccharide DNA aptamer–C1qrs complexes, Folia Microbiol. 53 (2008) 295–302.
[26] A. Wen, Q. Yang, J. Li, F. Lv, Q. Zhong, C. Chen, A novel lipopolysaccharide-antagonizing aptamer protects mice against endotoxemia, Biochem. Biophys. Res. Commun. 382 (2009) 140–144.
[27] H. Cai, T.M.-H. Lee, I.M. Hsing, Label-free protein recognition using an aptamer-based impedance measurement assay, Sens. Actuators B 114 (2006) 433–437.
[28] Y. Xu, L. Yang, X. Ye, P. He, Y. Fang, An aptamer-based protein biosensor by detecting the amplified impedance signal, Electroanalysis 18 (2006) 1449–1456.
[29] A. Sassolas, L.J. Blum, B.D. Leca-Bouvier, Electrochemical aptasensors, Electroanalysis 21 (2009) 1237–1250.
[30] A. Merkoci, M. Pumera, X. Llopis, B. Perez, M. Delvalle, S. Alegret, New materials for electrochemical sensing VI: carbon nanotubes, TrAC Trends Anal. Chem. 24 (2005) 826–838.
[31] M.K. Patel, P.R. Solanki, A. Kumar, S. Khare, S. Gupta, B.D. Malhotra, Electrochemical DNA sensor for Neisseria meningitidis detection, Biosens. Bioelectron. 25 (2010) 2586–2591.
[32] J.Y. Heras, D. Pallarola, F. Battaglini, Electronic tongue for simultaneous detection of endotoxins and other contaminants of microbiological origin, Biosens. Bioelectron. 25 (2010) 2470–2476.
[33] J.-D. Qiu, R.-P. Liang, R. Wang, L.-X. Fan, Y.-W. Chen, X.-H. Xia, A label-free amperometric immunosensor based on biocompatible conductive redox chitosan-ferrocene/gold nanoparticles matrix, Biosens. Bioelectron. 25 (2009) 852–857.
[34] M.J. Shin, L. Tan, M.H. Jeong, J.H. Kim, W.S. Choe, Monolith-based immobilized metal affinity chromatography increases production efficiency for plasmid DNA purification, J. Chromatogr. A 1218 (2011) 5273–5278.
[35] W. Lee, B.K. Oh, W.H. Lee, J.W. Choi, Immobilization of antibody fragment for immunosensor application based on surface plasmon resonance, Colloids Surf. B 40 (2005) 143–148.
[36] W.Q. Su, H.T. Nguyen, M.S. Cho, Y.K. Son, Y.K. Lee, Synthesis, characterization and self-assembled film of poly(3-((2,3-dihydrothieno[3,4-b][1,4]dioxin-2-yl)methoxy)propane-1-thiol) (PEDTMSHA), Synth. Met. 160 (2010) 2471–2475.
[37] T.M. Herne, M.J. Tarlov, Characterization of DNA probes immobilized on gold surfaces, J. Am. Chem. Soc. 119 (1997) 8916–8920.
[38] M. Zuker, Mfold web server for nucleic acid folding and hybridization prediction, Nucleic Acids Res. 31 (2003) 3406–3415.
[39] U.K. Sur, R. Subramanian, V. Lakshminarayanan, Cyclic voltammetric and electrochemical impedance studies on the structure, adsorption kinetics, and barrier properties of some organic dithiol self-assembled monolayers on gold, J. Colloid Interface Sci. 266 (2003) 175–182.
[40] F. Lucarelli, Carbon and gold electrodes as electrochemical transducers for DNA hybridisation sensors, Biosens. Bioelectron. 19 (2004) 515–530.